Dynamical free energy based model for quantum decision making

Tanaka, Shigenori
Umegaki, Toshihito
Nishiyama, Akihiro
Kitoh-Nishioka, Hirotaka

(Citation)
Physica A: Statistical Mechanics and its Applications,605:127979

(Issue Date)
2022-11-01

(Resource Type)
journal article

(Version)
Version of Record

(URL)
https://hdl.handle.net/20.500.14094/0100476449

Physica A 605 (2022) 127979

Contents lists available at ScienceDirect

Physica A

journal homepage: www.elsevier.com/locate/physa

Dynamical free energy based model for quantum decision making

Shigenori Tanaka *, Toshihito Umegaki [1], Akihiro Nishiyama, Hirotaka Kitoh-Nishioka [2]

Graduate School of System Informatics, Department of Computational Science, Kobe University, 1-1 Rokkodai, Nada-ku, Kobe 657-8501, Japan

ARTICLE INFO

Article history:
Received 24 March 2022
Received in revised form 12 May 2022
Available online 28 July 2022

Keywords:
Decision making
Quantum dynamics
Free energy
Entropy
Prisoner's dilemma
Sure thing principle

ABSTRACT

We propose a quantum-mechanical framework to describe the dynamics of human decision making, where the interactions between the open quantum system of decision makers and its surrounding environment at given temperature are relevantly taken into account. The temporal evolution of quantum system is described in terms of the time-dependent density matrix, from which we can evaluate those thermodynamic functions such as internal energy, (von Neumann) entropy and (Helmholtz) free energy. In this study we rely on the symmetrical quasi-classical (SQC) windowing approach to numerically solve the non-adiabatic quantum dynamics. We then consider the Hamiltonians to formulate the Prisoner's Dilemma (PD) problem and calculate the population dynamics of the quantum states of two players' decisions, where some quantum coherence or interference effects are observed. The evaluated free energy tends to decrease toward the thermodynamic equilibrium value, thus driving the dynamics of quantum system between the Nash equilibrium and Pareto optimum states. The calculated entropy often shows a tendency of temporal decrease, thus indicating the emergence of order in the quantum system. We have also applied the present scheme to the issue of the violation of the sure thing principle and found its occurrence through explicit numerical simulations for the PD problem. The present study may provide a theoretical basis to connect the dynamics of quantum decision making to the free energy principle in cognitive science.

1. Introduction

Theoretical and computational approaches for rational decision making have mostly been based on the classical probability framework to describe the human cognition [1]. These conventional approaches with long history presume that people can derive inferences from the classical Bayes rule and decisions from the expected utility rule in a rational manner. However, these classical, Bayesian approaches to cognition have often been challenged empirically [2,3] by such experimental facts in decision making as those observed in the Prisoner's Dilemma (PD) problem and the two-stage gambling task [4]. Examples concerning the breakdown of the classical framework of cognitive science include

* Corresponding author.
E-mail address: tanaka2@kobe-u.ac.jp (S. Tanaka).
1 Center for Mathematical Modeling and Data Science, Osaka University, Osaka, 560-8531, Japan.
2 Department of Energy and Materials, Faculty of Science and Engineering, Kindai University, Osaka 577-8502, Japan.

https://doi.org/10.1016/j.physa.2022.127979

Table 1
Gains according to each prisoner's choice.

	$\|B:0\rangle$	$\|B:1\rangle$
$\|A:0\rangle$	A ··· 1 B ··· 1	A ··· 3 B ··· 0
$\|A:1\rangle$	A ··· 0 B ··· 3	A ··· 2 B ··· 2

the violation of the sure thing principle and the conjunction fallacy [4,5]. Thus, in order to overcome these difficulties associated with the classical probability theory, some novel approaches based on the quantum probability model have been proposed [6–18], where those quantum effects associated with interference, coherence and superposition in the system state are expected to play essential roles. Above all, a pioneering work was performed by Pothos and Busemeyer [7] in which they constructed a quantum probability model based on a Hilbert space representation and Schrödinger equation to provide a simple explanation for paradoxical findings in psychological tasks, and compared the calculated results concerning the violation of the sure thing principle with those obtained by the classical Markov model, thus demonstrating the superiority of quantum model.

Here, one may remark that any biological system is fundamentally open and cannot survive without contacts with environment. In order to take into account these natural circumstances in the framework of quantum theory for human cognition, we should make sure modeling in which the interactions between the quantum system and its surrounding environment are considered along with the associated issues concerning the effective "temperature" and the decoherence effects in quantum mechanics [19–21]. Actually, we see in the literature [22–26] some attempts toward the theoretical descriptions of decision making in terms of open system on the basis of quantum master equation. For example, Martinez-Martinez and Sanchez-Burillo [23] employed a Lindblad-type Markovian master equation to describe the quantum stochastic walks on networks for decision making, in which the mixing of quantum and dissipative or relaxational characters of system was managed in a heuristic way to account for the violation of the sure thing principle. There, the Hamiltonian was used exclusively to produce the quantum interference effect, while it should intrinsically govern the thermodynamic stability of the system as well.

The purpose of the present work is then to propose a novel thermodynamics-based model for open quantum system to describe the human decision making, where the entangled, non-Markovian dynamics of two players in the PD problem is considered at finite temperature. To realize the modeling, we rely on theoretical formulations that have been shown to be useful for the description of quantum dynamics in those molecular systems such as photosynthetic proteins [27–29]. Given relevant Hamiltonian, we borrow the mathematical formalism successful for microscopic molecular systems embedded in environment [20] to describe the macroscopic temporal behaviors of human cognition, while we employ "atomic units" in which the Planck constant $\hbar$, the Boltzmann constant k_B, and particle masses are taken to be unity so that those physical quantities such as energy, temperature, frequency and time are relevantly rescaled. In this manner, we can systematically construct nonequilibrium thermodynamics for the quantum dynamics of decision making, in which the internal energy, the von Neumann entropy and the Helmholtz free energy of the two-player quantum system are appropriately identified and evaluated. We may then make a reasonable connection between the present theory and the free energy principle [30,31] that has recently attracted much attention in various fields of cognitive science.

In the following parts of this article, we first give a theoretical formulation to model the PD problem in the framework of dissipative quantum dynamics of open systems, where the quantum system composed of entangled two players interacts with the environment composed of a set of harmonic oscillators at a temperature. The modeled quantum dynamics are solved in the present study in terms of the symmetrical quasi-classical (SQC) approach [27–29] that has been successful in the descriptions of quantum dissipative dynamics of molecular systems. We perform the computer simulations for a general model of PD problem along with an examination on the violation of the sure thing principle. Some complementary remarks are provided in Supplementary Material, in which a number of theoretical schemes [20,32–37] to describe the quantum dynamics of open systems are compared with the SQC method.

2. Theory

2.1. Model for quantum decision making

In the present work we consider the two-person Prisoner's Dilemma (PD) problem [4,7,11,23] as a typical model for decision making. We consider two prisoners (or game players), A and B, and their decisions, $|0\rangle$ to defect against the opponent and $|1\rangle$ to cooperate with the other. According to the combinations of their decision choices, each of them is modeled in this study to gain the points indicated in the payoff matrix shown in Table 1. For example, if A cooperates ($|A:1\rangle$ and B defects ($|B:0\rangle$), A wins 0 point and B wins 3 points.

No matter what the other player does, an individual player gains more when he/she defects. This makes defection the dominant option when the game is played only once against a given opponent, and corresponds to the existence of the

Nash equilibrium [11] for the case of $|A:0\rangle\ |B:0\rangle$. However, this state is not Pareto efficient and there is a Pareto optimal state [11] for the case of $|A:1\rangle\ |B:1\rangle$ in this PD game, where the sum of the two players' gains becomes maximum.

In the following we describe this PD problem in terms of quantum dynamics by employing the four bases as $|A:0\rangle|B:0\rangle$, $|A:1\rangle|B:0\rangle$, $|A:0\rangle|B:1\rangle$ and $|A:1\rangle|B:1\rangle$ to denote the system states. Then, we can introduce the Hamiltonians $\hat{H}_{\rm A}$ and $\hat{H}_{\rm B}$ for the players A and B, respectively, in which the negatives of the payoff points are used for the diagonal elements of the Hamiltonian matrices to bring about an energetic stabilization of system in the thermodynamic equilibrium state. In addition, we can account for the off-diagonal elements of the Hamiltonian matrices to represent the quantum interference or state coupling effects as follows. First, we consider the inversion of either one player's choice as

$$\begin{aligned}
&|A:0\rangle|B:0\rangle \leftrightarrow |A:0\rangle|B:1\rangle,\\
&|A:0\rangle|B:0\rangle \leftrightarrow |A:1\rangle|B:0\rangle,\\
&|A:1\rangle|B:1\rangle \leftrightarrow |A:1\rangle|B:0\rangle,\\
&|A:1\rangle|B:1\rangle \leftrightarrow |A:0\rangle|B:1\rangle,
\end{aligned} \tag{1}$$

which are expressed in terms of Δ_s. Next, we may consider the simultaneous reversal of common choices of two players as

$$|A:0\rangle|B:0\rangle \leftrightarrow |A:1\rangle|B:1\rangle, \tag{2}$$

which is expressed by Δ_d. Finally, we may consider the exchange of two players' different choices as

$$|A:0\rangle|B:1\rangle \leftrightarrow |A:1\rangle|B:0\rangle, \tag{3}$$

which is expressed by Δ_e.

Thus, we can adopt the Hamiltonians for the players A and B as

$$\hat{H}_{\rm A} = \begin{pmatrix} -1 & \Delta_s & \Delta_s & \Delta_d \\ \Delta_s & 0 & \Delta_e & \Delta_s \\ \Delta_s & \Delta_e & -3 & \Delta_s \\ \Delta_d & \Delta_s & \Delta_s & -2 \end{pmatrix} \tag{4}$$

$$\hat{H}_{\rm B} = \begin{pmatrix} -1 & \Delta_s & \Delta_s & \Delta_d \\ \Delta_s & -3 & \Delta_e & \Delta_s \\ \Delta_s & \Delta_e & 0 & \Delta_s \\ \Delta_d & \Delta_s & \Delta_s & -2 \end{pmatrix} \tag{5}$$

respectively. By combining these two Hamiltonians, we can construct the Hamiltonian for the system composed of two players as

$$\hat{H}_{\rm S} = \theta\hat{H}_{\rm A} + (1-\theta)\hat{H}_{\rm B}, \quad (0 \le \theta \le 1) \tag{6}$$

where a weight parameter θ representing the relative significance of two players has been introduced.

In the framework of the PD problem, we are also interested in the issue of the violation of the sure thing principle [4], which may be associated with the quantum interference effect. The violation of the sure thing principle is known to be an example of the disjunction effect [3] in decision making, and was analyzed quantum mechanically by Pothos and Busemeyer [7]. As remarked by Shafir and Tversky [2] through cognitive experiments, many players defected knowing that the opponent defected or cooperated, whereas they switched and decided to cooperate when they did not know the opponent's action. This preference reversal by many players caused the proportion of defections for the unknown condition to fall below the proportions observed under the known conditions. Here, we consider two Hamiltonians for the player A (a special case of $\theta = 1$ in Eq. (6)) as

$$\hat{H}_0 = \begin{pmatrix} -1 & \Delta & 0 & 0 \\ \Delta & 0 & 0 & 0 \\ 0 & 0 & 0 & 0 \\ 0 & 0 & 0 & 0 \end{pmatrix} \tag{7}$$

$$\hat{H}_1 = \begin{pmatrix} 0 & 0 & 0 & 0 \\ 0 & 0 & 0 & 0 \\ 0 & 0 & -3 & \Delta \\ 0 & 0 & \Delta & -2 \end{pmatrix} \tag{8}$$

to describe the quantum dynamics of decision making of the player A when he/she knows that the player B has decided to defect or cooperate, respectively. Thus, the system Hamiltonian with inclusion of state coupling Δ is expressed by

$$\hat{H}_{\rm S} = \hat{H}_0 + \hat{H}_1, \tag{9}$$

representing the decomposition of quantum dynamics of the player A into two independent subspaces for which the decision of the player B has been fixed. On the other hand, when the player A does not know the decision of the player

B, the system Hamiltonian is perturbed so that the decision of the player A may be altered. We consider in the present study the addition of a perturbing Hamiltonian as

$$\hat{H}_{\mathrm{W}} = \begin{pmatrix} -\delta & 0 & -\delta & 0 \\ 0 & \delta & 0 & -\delta \\ -\delta & 0 & \delta & 0 \\ 0 & -\delta & 0 & -\delta \end{pmatrix} \tag{10}$$

which represents the effect of *wishful thinking* [2,4,7] with the parameter δ; that is, the players may tend to change their beliefs to be consistent with their own action. In the case of the PD game, if a player chooses to cooperate (defect), then he/she would tend to think that the opponent will cooperate (defect) as well. Moreover, in the present investigation we also consider an alternative perturbing (state mixing) Hamiltonian as

$$\hat{H}_{\mathrm{M}} = \begin{pmatrix} 0 & 0 & -\delta & 0 \\ 0 & 0 & 0 & -\delta \\ -\delta & 0 & 0 & 0 \\ 0 & -\delta & 0 & 0 \end{pmatrix} \tag{11}$$

which takes into account only the off-diagonal elements of $\hat{H}_{\mathrm{W}}$ to exclusively represent the quantum interference effect in terms of the state coupling. These Hamiltonians, $\hat{H}_{\mathrm{W}}$ and $\hat{H}_{\mathrm{M}}$, may be added to the system Hamiltonian given by Eq. (9) when we consider the possibility for the violation of the sure thing principle. It is noted in passing that the form of these system Hamiltonians is analogous to that employed for the transverse-field Ising model associated with the quantum annealing [38].

Next, we consider the coupling of the two-person quantum system to its surrounding environment. The environment is modeled in this study in terms of a set of quantum-mechanical harmonic oscillators or phonons in the equilibrium state at temperature T [19–21]. Thus, we consider the total Hamiltonian:

$$\hat{H} = \hat{H}_{\mathrm{S}} + \hat{H}_b + \hat{H}_c \tag{12}$$

with

$$\hat{H}_S = \sum_i \epsilon_i |i\rangle\langle i| + \sum_{i\neq j} \Delta_{ij} |i\rangle\langle j|, \tag{13}$$

$$\hat{H}_b = \frac{1}{2} \sum_{i,\xi} (\hat{P}_{i\xi}^2 + \omega_{i\xi}^2 \hat{R}_{i\xi}^2) |i\rangle\langle i|, \tag{14}$$

and

$$\hat{H}_c = -\sum_{i,\xi} c_{i\xi} \hat{R}_{i\xi} |i\rangle\langle i|. \tag{15}$$

In Eq. (13), $|i\rangle$, ϵ_i and Δ_{ij} refer to the quantum states (bases) of two players, the site energies (negatives of payoff points) and the off-diagonal elements (inter-state couplings) of the system Hamiltonian, respectively. $\hat{H}_b$ denotes the bath Hamiltonian of the harmonic oscillators with the frequencies $\omega_{i\xi}$ expressed by the quantum-mechanical momentum and coordinate operators, $\hat{P}_{i\xi}$ and $\hat{R}_{i\xi}$, of mode ξ at the site (state) i. $\hat{H}_c$ refers to the system-environment coupling Hamiltonian with the coupling constants $c_{i\xi}$.

In this way, we can describe the quantum dynamics of the two-person system embedded in the environment in terms of the time-dependent density operator or matrix. The density matrix $\hat{\rho}_{\mathrm{tot}}(t)$ for the total system obeys the Liouville–von Neumann equation [20] as

$$\frac{\partial}{\partial t} \hat{\rho}_{\mathrm{tot}}(t) = \frac{1}{i} [\hat{H}, \hat{\rho}_{\mathrm{tot}}(t)], \tag{16}$$

which can be solved with relevant initial condition $\hat{\rho}_{\mathrm{tot}}(0)$. The dissipative dynamics of the quantum system is then described in terms of the reduced density matrix that can be obtained by tracing out the environmental degrees of freedom (DOF) in $\hat{\rho}_{\mathrm{tot}}(t)$. In general, the theoretical formulation based on the model Hamiltonian, Eqs. (12)–(15), is very formal, so that the distinction between the system and its environment is fairly arbitrary.

2.2. Quantum dynamics

In order to numerically solve the quantum dynamics problem formulated in the preceding section, we rely on the symmetrical quasi-classical (SQC) windowing approach to the Meyer–Miller (MM) classical vibronic Hamiltonian [27–29]. The MM Hamiltonian [39] was originally developed to map the coupled dynamics of nuclear and electronic degrees of freedom (DOF) in non-adiabatic processes onto a set of classical "electronic" oscillators with each oscillator representing the occupation of the various electronic states. The SQC/MM method has provided excellent descriptions of a variety

of electronically non-adiabatic benchmark model systems for which exact or accurate quantum results are available for comparison [32,33,36,37].

The original SQC/MM methodology [27–29] thus consists of two basic ingredients such as the MM *classical* Hamiltonian to treat nuclear and electronic DOF in a consistent unified framework and the SQC windowing procedure used to "quantize" the electronic DOF embodied as classical oscillators in the MM Hamiltonian, that is a kind of Bohr–Sommerfeld quantization of classical action variables. Each electronic state's occupation is described by a classical harmonic oscillator, and the first excited state and the ground state of each oscillator represent whether the corresponding electronic state is occupied or unoccupied, respectively. Then, regarding the system and environment DOF in the present study as the electronic and nuclear DOF, respectively, the MM Hamiltonian is expressed as

$$H(\boldsymbol{P},\boldsymbol{R},\boldsymbol{p},\boldsymbol{x}) = \frac{\boldsymbol{P}^2}{2} + \sum_{k=1}^{n_{\rm state}} \left(\frac{p_k^2}{2} + \frac{x_k^2}{2} - \gamma\right) H_{k,k}(\boldsymbol{R}) + \sum_{k<k'=1}^{n_{\rm state}} (p_k p_{k'} + x_k x_{k'})\, H_{k,k'}(\boldsymbol{R}), \tag{17}$$

where $\{p_k, x_k\}$ are the momenta and coordinates of quantum (system) oscillators ($k = 1, 2, \ldots, n_{\rm state}$), and $\{\boldsymbol{P}, \boldsymbol{R}\}$ refer to the momenta and coordinates of bath (environment) oscillators; $H_{k,k}(\boldsymbol{R})$ and $H_{k,k'\neq k}(\boldsymbol{R})$ refer to the diabatic system potential energy surface (PES) for the state k and the non-adiabatic inter-state couplings, respectively, which are parametrically dependent on the environmental coordinates $\boldsymbol{R}$; γ is a fixed zero-point energy parameter, which will be specified later. In addition, an equivalent expression in terms of classical harmonic-oscillator action–angle variables for the system is given by

$$H(\boldsymbol{P},\boldsymbol{R},\boldsymbol{n},\boldsymbol{q}) = \frac{\boldsymbol{P}^2}{2} + \sum_{k=1}^{n_{\rm state}} n_k H_{k,k}(\boldsymbol{R}) + 2\sum_{k<k'=1}^{n_{\rm state}} \sqrt{(n_k+\gamma)(n_{k'}+\gamma)}\cos(q_k - q_{k'}) H_{k,k'}(\boldsymbol{R}). \tag{18}$$

Here, the Cartesian $\{p_k, x_k\}$ and action–angle $\{n_k, q_k\}$ variables of the system are related by the canonical transformation as

$$p_k = -\sqrt{2\,(n_k+\gamma)}\,\sin q_k, \tag{19}$$

$$x_k = \sqrt{2\,(n_k+\gamma)}\,\cos q_k, \tag{20}$$

or inversely,

$$n_k = \frac{p_k^2}{2} + \frac{x_k^2}{2} - \gamma, \tag{21}$$

$$q_k = -\tan^{-1}\frac{p_k}{x_k}. \tag{22}$$

Since the system state (or site) $|k\rangle$ is non-adiabatically coupled to each other and also coupled to the harmonic bath particular to that state in the present model, the diagonal PES part in the MM Hamiltonian above can be written as

$$H_{k,k}(\boldsymbol{R}) = \epsilon_k + h_b^{(k)}(\boldsymbol{P}, \boldsymbol{R}-\boldsymbol{D}) + \sum_{k'\neq k} h_b^{(k')}(\boldsymbol{P},\boldsymbol{R}) \tag{23}$$

with the bath Hamiltonian

$$h_b^{(k)}(\boldsymbol{P},\boldsymbol{R}) = \frac{1}{2}\sum_{\xi\in \text{site } k} (P_\xi^2 + \omega_\xi^2 R_\xi^2). \tag{24}$$

It is noted here that the bath coordinates for the state $|k\rangle$ are shifted by

$$D_\xi^{(k)} = c_{k\xi}/\omega_{k\xi}^2 \tag{25}$$

due to the system–bath coupling given by Eq. (15). On the other hand, the off-diagonal part $H_{k,k'\neq k}(\boldsymbol{R})$ in the MM Hamiltonian comes only from the coupling constants $\Delta_{kk'}$ in the system Hamiltonian, Eq. (13).

The system–bath coupling significantly affects the quantum dynamics of the system that is modeled as a PD problem in the present study. The bath is modeled as a set of quantum-mechanical harmonic oscillators coupled to each quantum state $|k\rangle$, and their thermal distribution is initially given by

$$\rho_b^{(k)}(\boldsymbol{P},\boldsymbol{R}) \propto \prod_{\xi\in \text{site } k}^{n_{\rm osc}} \exp\left[-\frac{\alpha_\xi}{2}\left(P_\xi^2 + \omega_\xi^2 R_\xi^2\right)\right] \tag{26}$$

with

$$\alpha_\xi = \frac{2}{\omega_\xi}\tanh\left(\frac{\beta\omega_\xi}{2}\right)\ (\xi = 1, \ldots, n_{\rm osc}), \tag{27}$$

where each mode ξ coupled to the state $|k\rangle$ is assumed to be in thermal equilibrium at inverse temperature $\beta = 1/T$. In the following analysis, as an optional case, the system–bath coupling is described in terms of the Debye-type spectral density [28] as

$$J(\omega) = 2\lambda\frac{\omega\omega_c}{\omega^2 + \omega_c^2} \tag{28}$$

with the reorganization energy

$$\lambda = \frac{1}{2}\sum_{\xi\in{\rm site}\ k}\omega_\xi^2 D_\xi^2 = \frac{1}{\pi}\int_0^\infty \frac{d\omega}{\omega}J(\omega) \tag{29}$$

and the characteristic frequency ω_c. Given the spectral density, the bath coordinate shifts are obtained by

$$D_\xi = \sqrt{\frac{2}{\pi}J(\omega_\xi)\Delta\omega/\omega_\xi^3}, \tag{30}$$

where $\Delta\omega = \omega_\xi - \omega_{\xi-1}$ with $\omega_0 = 0$ and the discretized (incremental) distribution of bath frequencies ω_ξ can be obtained according to an optimal prescription given in the literature [40,41].

In this way, given the classical MM Hamiltonian, Eq. (17) or (18), the coupled dynamics of system–bath DOF is described by solving the Hamilton equations, $d\boldsymbol{p}/dt = -\partial H/\partial\boldsymbol{x}$, $d\boldsymbol{x}/dt = \partial H/\partial\boldsymbol{p}$, $d\boldsymbol{P}/dt = -\partial H/\partial\boldsymbol{R}$, and $d\boldsymbol{R}/dt = \partial H/\partial\boldsymbol{P}$.

Then, the reduced density matrix for the quantum state $|i\rangle$ can be calculated as follows in the framework of SQC/MM scheme [27–29,42]. We consider the window function, $\hat\delta(n)$, which takes a value of unity when the action variable n falls in a window region specified around the origin (zero value). The unnormalized, reduced density matrix is then expressed by

$$\rho_{ii}(t) = \hat\delta(n_i - 1)\prod_{k\neq i}\hat\delta(n_k) \tag{31}$$

for the diagonal elements and

$$\rho_{ij}(t) = \exp\left[-i(q_i - q_j)\right]\hat\delta\left(n_i - \frac{1}{2}\right)\hat\delta\left(n_j - \frac{1}{2}\right)\prod_{k\neq i,j}\hat\delta(n_k) \tag{32}$$

for the off-diagonal elements by using the action and angle coordinates calculated at time t. We employ in this study the rectangular window with the width $\gamma = (\sqrt{3} - 1)/2 = 0.366$ for the window function. After making the ensemble average (that is, sampling over the randomized initial conditions and averaging over multiple classical trajectories) and the normalization as

$$\sum_{i=1}^{n_{\rm state}}\rho_{ii}(t) = 1, \tag{33}$$

we obtain each element of the reduced density matrix for the state $|i\rangle$.

Given the total Hamiltonian, Eq. (12), the present approach to solve the dissipative quantum dynamics based on the SQC scheme is nearly exact (see Supplementary Material), and provides very accurate descriptions of non-Markovian temporal evolution of quantum states beyond the Lindblad scheme [20] that approximately treats the quantum system weakly coupled to Markovian reservoir.

2.3. Thermodynamics

After having obtained the reduced density matrix $\hat\rho(t)$ for the two-person system embedded in the environmental bath at temperature T, we can evaluate the Helmholtz free energy:

$$F(t) = U(t) - TS(t) \tag{34}$$

as a function of time t. Here,

$$U(t) = {\rm Tr}\left[\hat\rho(t)\hat H_{\rm S}\right] \tag{35}$$

is the internal energy and

$$S(t) = -{\rm Tr}\left[\hat\rho(t)\ln\hat\rho(t)\right] \tag{36}$$

is the von Neumann entropy, in which Tr refers to the trace and ${\rm Tr}\hat\rho(t) = 1$.

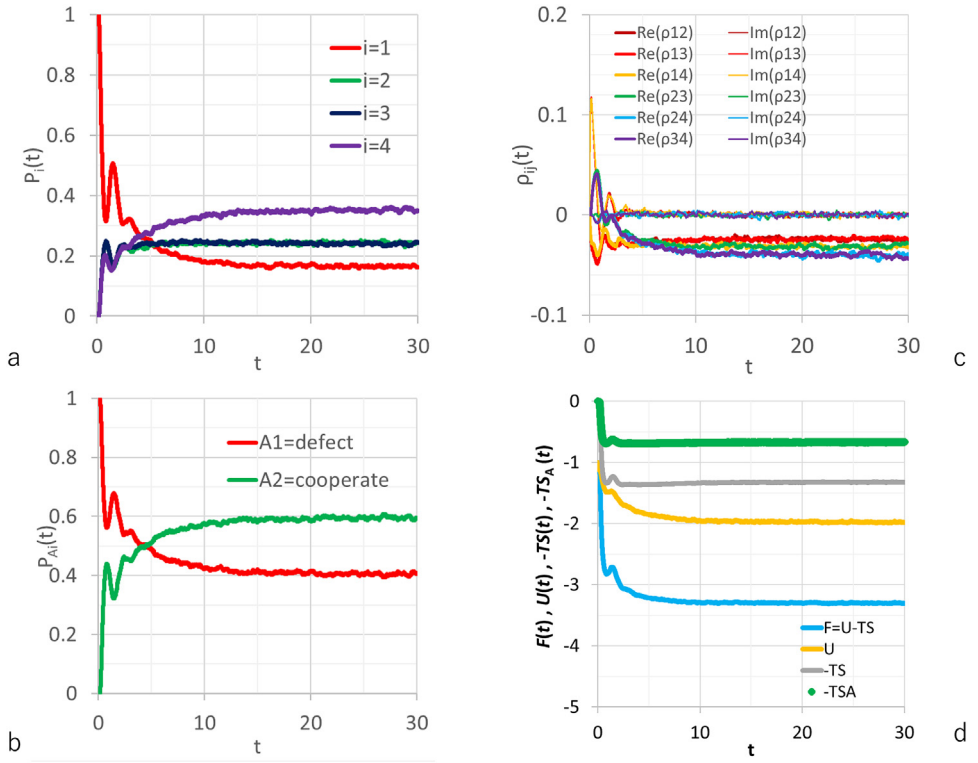

Fig. 1. (a) Population dynamics calculated for the PD problem with $\theta = 1/2$ and $\Delta = 1$ when the initial condition is $P_1(0) = 1$ and $P_2(0) = P_3(0) = P_4(0) = 0$, where the Debye-type spectral density, Eq. (28), is employed with $\lambda = 1$ and $\omega_c = 1$ at $T = 1$. Red, green, black and purple lines refer to the temporal evolutions of $P_i(t)$ for $i = 1, 2, 3$ and 4, respectively. (b) Temporal evolution of the decision probability of player A; red and green lines refer to the calculated results for defection and cooperation. (c) Temporal evolutions of the off-diagonal elements of density matrix, $\rho_{ij}(t)$; thick and thin lines illustrate the calculated results for the real and imaginary parts, respectively, where different colors denoted in the inset are used for each element. (d) Temporal evolutions of the thermodynamic functions; yellow, gray, blue and green lines refer to the results for the internal energy $U(t)$, the von Neumann entropy $S(t)$ (times $-T$), the Helmholtz free energy $F(t)$ and the entanglement entropy $S_A(t)$ (times $-T$), respectively.

When $t \to \infty$, the system approaches the thermodynamic equilibrium state as described by the equilibrium density matrix as

$$\hat{\rho}_{\rm eq} = \frac{e^{-\beta \hat{H}_S}}{{\rm Tr}\left(e^{-\beta \hat{H}_S}\right)}. \tag{37}$$

We can prove that the equilibrium free energy $F_{\rm eq}$ gives the minimum value, as shown by

$$\beta F - \beta F_{\rm eq} = {\rm Tr}\left[\hat{\rho}(\ln \hat{\rho} - \ln \hat{\rho}_{\rm eq})\right] \geq {\rm Tr}\left(\hat{\rho} - \hat{\rho}_{\rm eq}\right) = 0, \tag{38}$$

where Klein's inequality [43] has been employed. This is the quantum version of the corresponding classical–mechanical relationship [44] and gives the underlying dynamical principle toward the thermal equilibrium of the system at temperature T.

Furthermore, we may evaluate the degree of entanglement between the two-player states in the present PD problem. When we have a wavefunction for the two-person (A and B) system represented by

$$|\psi\rangle = \sum_{x \in {\rm A}} \sum_{y \in {\rm B}} \psi(x, y)|x\rangle \otimes |y\rangle, \tag{39}$$

the density matrix of the system (pure state) is expressed by

$$\hat{\rho} = |\psi\rangle\langle\psi| = \sum_{x,x' \in A} \sum_{y,y' \in B} \psi(x, y)\psi^*(x', y')|x\rangle \otimes |y\rangle\langle y'| \otimes \langle x'|. \tag{40}$$

Then, introducing

$$\rho(x; y, x'; y') = \psi(x, y)\psi^*(x', y'), \tag{41}$$

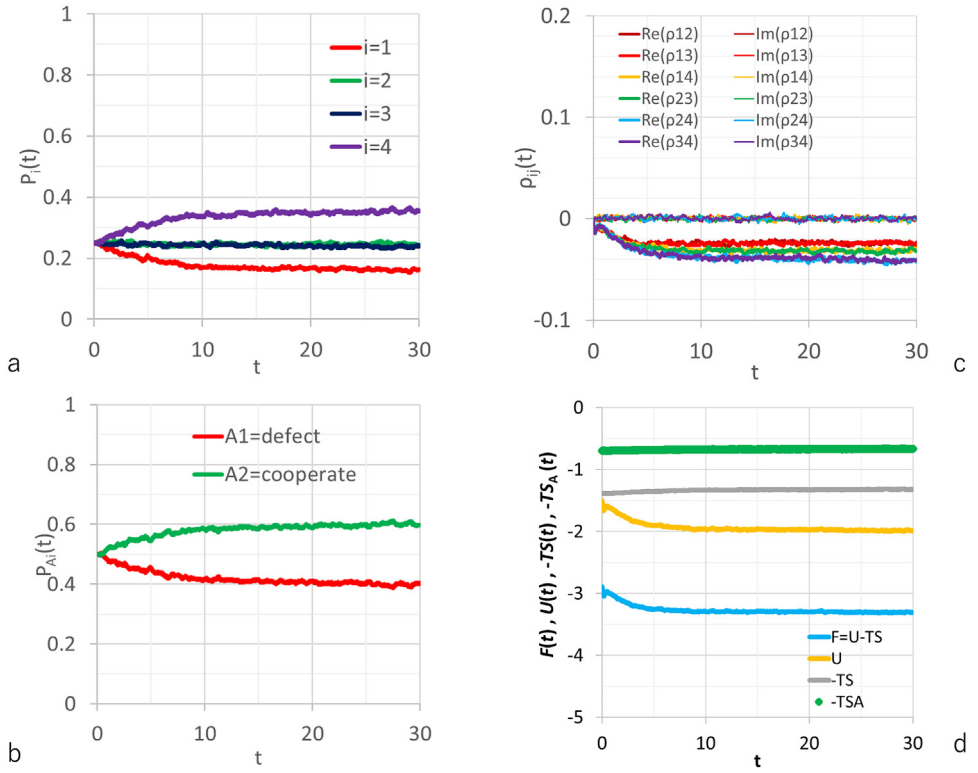

Fig. 2. (a) Population dynamics calculated for the PD problem with $\theta = 1/2$ and $\Delta = 1$ when the initial condition is $P_1(0) = P_2(0) = P_3(0) = P_4(0) = 1/4$, where the Debye-type spectral density, Eq. (28), is employed with $\lambda = 1$ and $\omega_c = 1$ at $T = 1$. Red, green, black and purple lines refer to the temporal evolutions of $P_i(t)$ for $i = 1, 2, 3$ and 4, respectively. (b) Temporal evolution of the decision probability of player A; red and green lines refer to the calculated results for defection and cooperation. (c) Temporal evolutions of the off-diagonal elements of density matrix, $\rho_{ij}(t)$; thick and thin lines illustrate the calculated results for the real and imaginary parts, respectively, where different colors denoted in the inset are used for each element. (d) Temporal evolutions of the thermodynamic functions; yellow, gray, blue and green lines refer to the results for the internal energy $U(t)$, the von Neumann entropy $S(t)$ (times $-T$), the Helmholtz free energy $F(t)$ and the entanglement entropy $S_A(t)$ (times $-T$), respectively.

the density matrices for the subsystems A and B are given by

$$\rho_A(x, x') = \sum_{y \in B} \rho(x; y, x'; y), \tag{42}$$

$$\rho_B(y, y') = \sum_{x \in A} \rho(x; y, x; y'). \tag{43}$$

Entanglement entropy [45,46] of the subsystem A is then obtained by

$$S_A = -\mathrm{Tr}_A\,(\rho_A \ln \rho_A) = -\sum_i p_i \ln p_i, \tag{44}$$

where p_i is eigenvalues of the matrix ρ_A. The procedures in Eqs. (42)–(44) can also be applied to the mixed states of quantum systems. The entanglement entropy has a property of $S_A = S_B$ and represents how much the quantum state of a system deviates from that expressed by the direct product of the subsystems.

In the thermodynamic formalism illustrated above, the distinction between the open quantum system and its environment is fairly arbitrary. Starting with Eqs. (12)–(15) for the total Hamiltonian, we can systematically construct the dynamical thermodynamic theory for the open quantum system without procedural ambiguity or further model tuning, which can be regarded as an advantage of the present theory over earlier studies [22–26] in which the quantum and stabilization issues were individually described by Hamiltonian and jump operators in Lindblad equation, respectively. In the present approach to the PD problem, the system represents the entangled decisions of two players whose Hamiltonian is given by $\hat{H}_S$ of Eq. (6), and then the environment refers to those fluctuating disturbances to affect the decision making of the players such as their knowledge, memory, belief, mood, physical or emotional states, other people's opinions and interference with other tasks. The degree of the environmental fluctuations is measured by the "temperature" T and the strength of the interactions between the system and environment is represented by the reorganization energy λ in the present harmonic oscillator based model (see Eqs. (28) and (29)). The diagonal elements of the system Hamiltonian $\hat{H}_S$ are

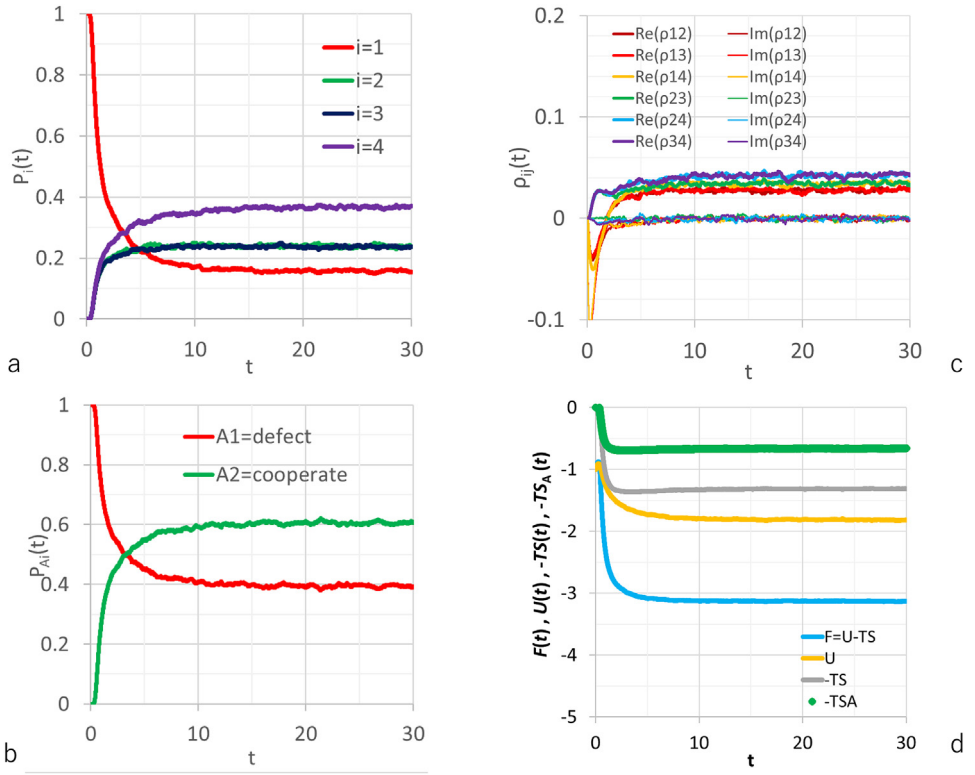

Fig. 3. (a) Population dynamics calculated for the PD problem with $\theta = 1/2$ and $\Delta = -0.5$ when the initial condition is $P_1(0) = 1$ and $P_2(0) = P_3(0) = P_4(0) = 0$, where the Debye-type spectral density, Eq. (28), is employed with $\lambda = 1$ and $\omega_c = 1$ at $T = 1$. Red, green, black and purple lines refer to the temporal evolutions of $P_i(t)$ for $i = 1, 2, 3$ and 4, respectively. (b) Temporal evolution of the decision probability of player A; red and green lines refer to the calculated results for defection and cooperation. (c) Temporal evolutions of the off-diagonal elements of density matrix, $\rho_{ij}(t)$; thick and thin lines illustrate the calculated results for the real and imaginary parts, respectively, where different colors denoted in the inset are used for each element. (d) Temporal evolutions of the thermodynamic functions; yellow, gray, blue and green lines refer to the results for the internal energy $U(t)$, the von Neumann entropy $S(t)$ (times $-T$), the Helmholtz free energy $F(t)$ and the entanglement entropy $S_A(t)$ (times $-T$), respectively.

given by the negatives of the payoffs (site energies ϵ_i) which direct the population probability of each quantum state in proportion to $\exp(-\epsilon_i/T)$ (neglecting the contribution from the off-diagonal elements, see also Supplementary Material) for the thermodynamic equilibrium ($t \to \infty$), thus stabilizing the system states asymptotically; the off-diagonal elements of $\hat{H}_S$, on the other hand, describe the quantum interference or coherence effects between the quantum states, which could cause the oscillation of the population probabilities of players' decision. It is noted that the system simultaneously has a thermal distribution in decision states through the interaction with environment, which determines the system entropy S expressing the degree of uncertainty (order or disorder) in the distribution of decision states. Given the internal energy $U = \langle \hat{H}_S \rangle$, entropy S and temperature T, the free energy is evaluated by $F = U - TS$. The essential thing in the present formalism is that this Helmholtz free energy determines the thermodynamically stable states and the principle of its minimalization governs the system dynamics (see Eq. (38)). Thus, the present formalism can provide a quantum model for decision making that may embody the free energy principle advocated by Friston [30,31] in a statistical–mechanically consistent manner.

3. Results and discussion

3.1. PD problem

In this section, we consider the PD problem whose system Hamiltonian is given by Eq. (6). As a prototypical example, we consider the case of $\theta = 1/2$ which means that the two players A and B are treated equally. In addition, we here assume that all the coupling constants in Eqs. (4) and (5) take an identical value, Δ, for simplicity. Environmental temperature is set to be $T = 1$, and in the Debye-type spectral density in Eq. (28) the reorganization energy and the characteristic frequency are taken to be $\lambda = 1$ and $\omega_c = 1$, respectively.

We employ the SQC methodology to describe the system dynamics. The rectangular windows are used with the zero-point energy parameter $\gamma = 0.366$ and $n_{\mathrm{osc}} = 400$ harmonic oscillators are coupled to each system state. Ensemble

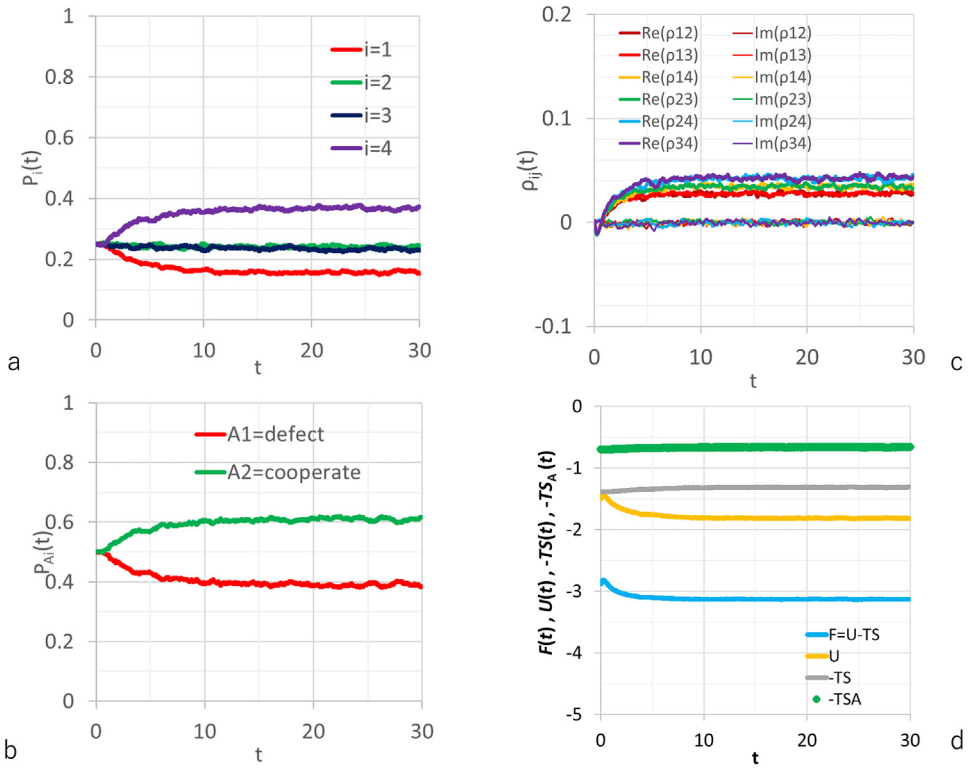

Fig. 4. (a) Population dynamics calculated for the PD problem with $\theta = 1/2$ and $\Delta = -0.5$ when the initial condition is $P_1(0) = P_2(0) = P_3(0) = P_4(0) = 1/4$, where the Debye-type spectral density, Eq. (28), is employed with $\lambda = 1$ and $\omega_c = 1$ at $T = 1$. Red, green, black and purple lines refer to the temporal evolutions of $P_i(t)$ for $i = 1, 2, 3$ and 4, respectively. (b) Temporal evolution of the decision probability of player A; red and green lines refer to the calculated results for defection and cooperation. (c) Temporal evolutions of the off-diagonal elements of density matrix, $\rho_{ij}(t)$; thick and thin lines illustrate the calculated results for the real and imaginary parts, respectively, where different colors denoted in the inset are used for each element. (d) Temporal evolutions of the thermodynamic functions; yellow, gray, blue and green lines refer to the results for the internal energy $U(t)$, the von Neumann entropy $S(t)$ (times $-T$), the Helmholtz free energy $F(t)$ and the entanglement entropy $S_A(t)$ (times $-T$), respectively.

average derived from random numbers is taken on 40000 independent trajectories to obtain the density matrices. We have performed the SQC calculations with our original code, while there is an open source code available at GitHub (https://github.com/jprov410/mqds) [47].

We first consider the case that the initial state is the Nash equilibrium state $|A:0\rangle\,|B:0\rangle$ and the coupling constant is $\Delta = 1$. Fig. 1 (a) shows the result for the population dynamics of the four states, $|A:0\rangle|B:0\rangle$, $|A:1\rangle|B:0\rangle$, $|A:0\rangle|B:1\rangle$ and $|A:1\rangle|B:1\rangle$. As is expected, the state of $|A:1\rangle|B:1\rangle$ which means that both players cooperate (a Paretian optimum) becomes dominant with the temporal evolution because this state corresponds to the lowest energy state in the system Hamiltonian $\hat{H}_S$ in the case of $\theta = 1/2$. The fractions of the four states finally approach those in the thermodynamic equilibrium at $T = 1$ (see also Supplementary Material). Interestingly, we observe the temporal oscillations of populations in short-time regime, which are associated with the quantum coherence or interference effects. Fig. 1 (b) then illustrates the temporal evolution of the decision of the player A, indicating a tendency of the transition from the initial defection to the final cooperation with the quantum beating. In addition to the population dynamics given by the diagonal elements of the density matrix, we illustrate in Fig. 1(c) the temporal evolution of the off-diagonal elements of the density matrix $\rho_{ij}(t)$, thus showing the emergence of quantum coherence caused by the coupling constants Δ.

Furthermore, the temporal evolutions of internal energy, entropy and free energy of the quantum system are shown in Fig. 1(d). The Helmholtz free energy tends to decrease toward the thermodynamic equilibrium value (see Eq. (38)), thus driving the quantum dynamics of decision-making system of two players. In Fig. 1(d) we also illustrate the behavior of the entanglement entropy for the subsystem of player A, which becomes almost constant in short time after the initial increase, since the initial state is expressed by a simple product of the defection states of two subsystems.

Next, when we choose the initial condition that the four quantum states are equally excited without coherence, that is, $\rho_{ii}(0) = 1/4$ $(i = 1, 2, 3, 4)$, we find the population dynamics of the four states as shown in Fig. 2(a). The corresponding temporal evolution of the decision of player A is then illustrated in Fig. 2(b), which indicates that the player A gradually tends to favor the cooperation. Concerning the quantum coherence, Fig. 2(c) shows the emergence of the off-diagonal

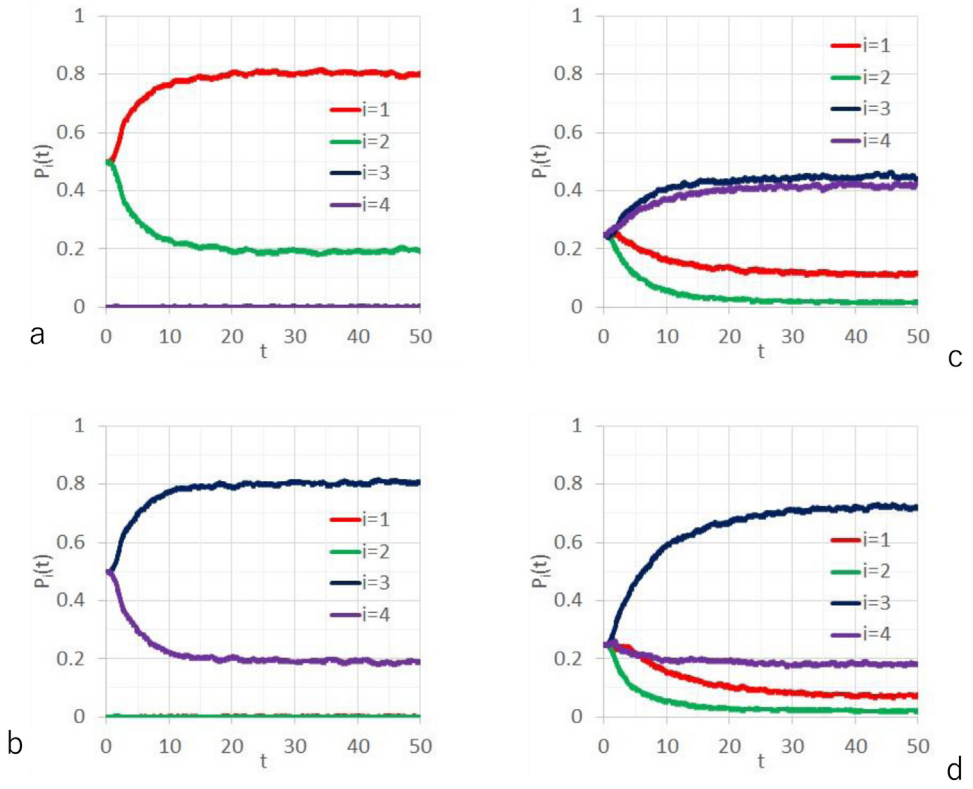

Fig. 5. (a) Population dynamics calculated for the Hamiltonian $\hat{H}_S$ given by Eq. (9) with $\Delta = -0.5$ when the initial condition is $P_1(0) = P_2(0) = 1/2$ and $P_3(0) = P_4(0) = 0$, where the Debye-type spectral density, Eq. (28), is employed with $\lambda = 0.5$ and $\omega_c = 1$ at $T = 0.5$. Red, green, black and purple lines refer to the temporal evolutions of $P_i(t)$ for $i = 1, 2, 3$ and 4, respectively. (b) Population dynamics calculated for the Hamiltonian $\hat{H}_S$ given by Eq. (9) with $\Delta = -0.5$ when the initial condition is $P_1(0) = P_2(0) = 0$ and $P_3(0) = P_4(0) = 1/2$, where other calculation parameters and color representations are the same as in (a). (c) Population dynamics calculated for the Hamiltonian $\hat{H}_S$ plus $\hat{H}_W$ with $\Delta = -0.5$ and $\delta = 0.5$ when the initial condition is $P_1(0) = P_2(0) = P_3(0) = P_4(0) = 1/4$, where other calculation parameters and color representations are the same as in (a). (d) Population dynamics calculated for the Hamiltonian $\hat{H}_S$ plus $\hat{H}_M$ with $\Delta = -0.5$ and $\delta = 0.5$ when the initial condition is $P_1(0) = P_2(0) = P_3(0) = P_4(0) = 1/4$, where other calculation parameters and color representations are the same as in (a).

elements of density matrix caused by the non-adiabatic coupling constants. Fig. 2 (d) shows the temporal evolutions of thermodynamic functions, where we observe the decreasing tendency of free energy as well as a slight temporal decrease of entropy, which means the emergence of order compared to the initial disorder (*i.e.*, equally distributed, mixed) state.

The non-adiabatic coupling constants may take negative signs in actual quantum systems [28]. We have therefore studied the case of $\Delta = -0.5$ as well as the simulations shown above. Fig. 3 (a) shows the results for the temporal evolutions of state populations when the Nash equilibrium $|A:0\rangle\ |B:0\rangle$ is taken to be the initial state. The calculated results are similar to those in Fig. 1(a), while the quantum beating is virtually invisible probably due to the reduced magnitude of the coupling constants. Similar behaviors are observed in Fig. 3(b) for the calculated result for the temporal evolution of the decision of player A. By contrast, the result for the temporal evolutions of the off-diagonal elements of density matrix shown in Fig. 3(c) indicates the inversion of the signs of the real parts due to that of the coupling constants. The behaviors of temporal evolutions of the thermodynamic functions illustrated in Fig. 3(d) are similar to those in Fig. 1(d). In addition, we also show the results obtained for the initial condition of equal populations of four states, $\rho_{ii}(0) = 1/4$ $(i = 1, 2, 3, 4)$, in Fig. 4. As is expected, Figs. 4(a), 4(b) and 4(d) show similar behaviors to those in Figs. 2(a), 2(b) and 2(d), respectively, while the signs of the real parts of the off-diagonal elements of density matrix shown in Fig. 4(c) are inverted (from negative to positive) compared to those in Fig. 2(c).

As has been shown in the calculated results above, the present theory and modeling can relevantly describe the dynamics of quantum decision making associated with the PD problem in terms of the entangled quantum system interacting with environmental thermal bath.

3.2. Violation of the sure thing principle

In this section, we proceed to the application of the present methodology to the issue of the violation of the sure thing principle. As addressed in Sec. 2.1, we consider the system Hamiltonian given by Eqs. (7)–(11) in this case. The simulation

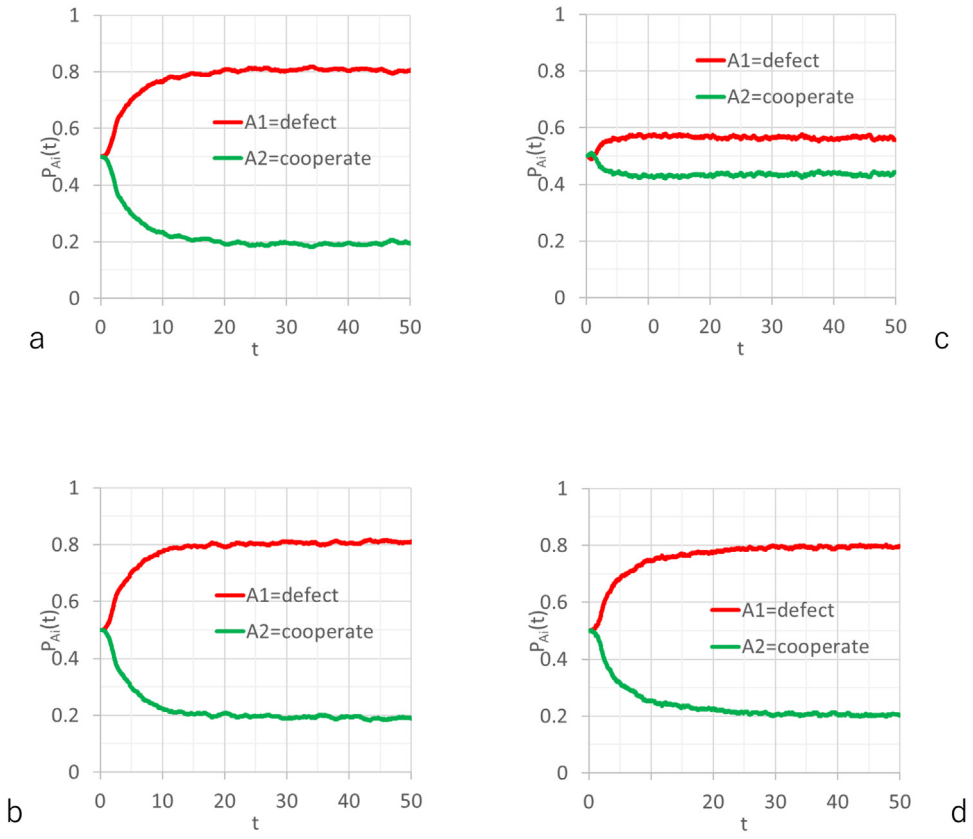

Fig. 6. Temporal evolution of the decision probability by player A concerning the violation of the sure thing principle. Red and green lines refer to the calculated results for defection and cooperation. (a) Result for the Hamiltonian $\hat{H}_S$ given by Eq. (9) with $\Delta = -0.5$ when the initial condition is $P_1(0) = P_2(0) = 1/2$ and $P_3(0) = P_4(0) = 0$, where the Debye-type spectral density, Eq. (28), is employed with $\lambda = 0.5$ and $\omega_c = 1$ at $T = 0.5$. (b) Result for the Hamiltonian $\hat{H}_S$ given by Eq. (9) with $\Delta = -0.5$ when the initial condition is $P_1(0) = P_2(0) = 0$ and $P_3(0) = P_4(0) = 1/2$, where other calculation parameters are the same as in (a). (c) Result for the Hamiltonian $\hat{H}_S$ plus $\hat{H}_W$ with $\Delta = -0.5$ and $\delta = 0.5$ when the initial condition is $P_1(0) = P_2(0) = P_3(0) = P_4(0) = 1/4$, where other calculation parameters are the same as in (a). (d) Result for the Hamiltonian $\hat{H}_S$ plus $\hat{H}_M$ with $\Delta = -0.5$ and $\delta = 0.5$ when the initial condition is $P_1(0) = P_2(0) = P_3(0) = P_4(0) = 1/4$, where other calculation parameters are the same as in (a).

method is analogous to that employed for the PD problem in the preceding section, while we use $\Delta = -0.5$, $\delta = 0.5$, $T = 0.5$ and $\lambda = 0.5$ to compare the present results to those in earlier studies [4,7].

We first consider the dynamics of the decision of player A when he/she knows the decision of player B. According to the decision of player B, the system Hamiltonian for the player A given by Eqs. (7)–(9) is decomposed into two subspaces expressed by $\hat{H}_0$ and $\hat{H}_1$. Fig. 5 (a) shows the temporal evolutions of quantum states when the player B is known to defect and the initial condition is $\rho_{11}(0) = \rho_{22}(0) = 1/2$ and $\rho_{33}(0) = \rho_{44}(0) = 0$; initially starting with the decision of player A being in the equal probability of defection and cooperation, he/she gradually tends to defect so that he/she will gain more payoff. This temporal change of the decision of player A is observed also in Fig. 6(a), in which the temporal evolutions of the probabilities of the defection and cooperation by player A are illustrated, and the time average of the probability of the defection by player A is found to be 0.776 over $t = 0 - 50$. On the other hand, when the player B is known to cooperate and the initial condition is $\rho_{11}(0) = \rho_{22}(0) = 0$ and $\rho_{33}(0) = \rho_{44}(0) = 1/2$, the corresponding results are illustrated in Figs. 5(b) and 6(b), again showing that the player A gradually tends to defect; the time average of the probability of the defection by player A is found to be 0.777 over $t = 0 - 50$.

Then, our interest is how much the probability of the defection by player A is changed when he/she does not know the decision of player B. With the addition of the "wishful thinking" Hamiltonian $\hat{H}_W$ to the system Hamiltonian $\hat{H}_S$, we have obtained the results for the population dynamics of four quantum states as shown in Fig. 5(c) starting from the initial condition of $\rho_{11}(0) = \rho_{22}(0) = \rho_{33}(0) = \rho_{44}(0) = 1/4$. The corresponding result concerning the decision of player A is illustrated in Fig. 6(c), thus giving a substantially lower value, 0.563, for the time average of the probability of the defection by player A over $t = 0 - 50$. Even when we employ the additional Hamiltonian $\hat{H}_M$ given by Eq. (11) instead of $\hat{H}_W$, we observe the reduction of the probability of the defection by player A, as illustrated in Figs. 5(d) and 6(d), giving 0.759 as the time average of the probability of the defection by player A over $t = 0 - 50$. Thus, we see a realization of the violation of the sure thing principle in our simulations for the quantum dynamics of decision making, in which

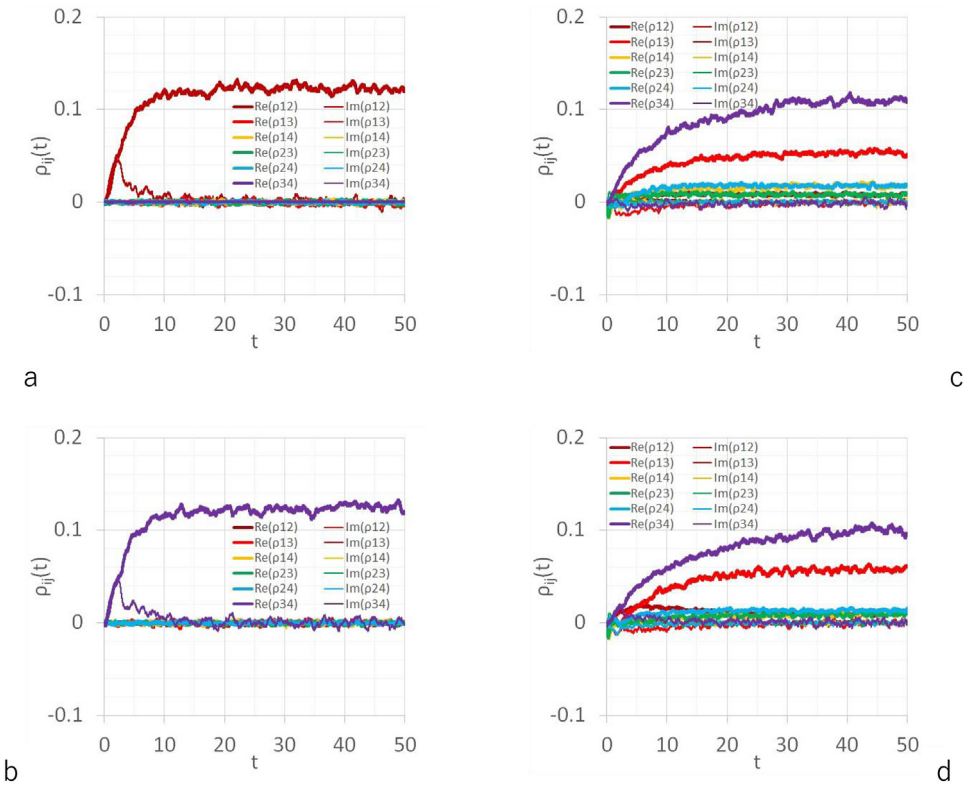

Fig. 7. Temporal evolutions of the off-diagonal elements of density matrix, $\rho_{ij}(t)$, concerning the violation of the sure thing principle. Thick and thin lines illustrate the calculated results for the real and imaginary parts, respectively, where different colors denoted in the inset are used for each element. (a) Result for the Hamiltonian $\hat{H}_S$ given by Eq. (9) with $\Delta = -0.5$ when the initial condition is $P_1(0) = P_2(0) = 1/2$ and $P_3(0) = P_4(0) = 0$, where the Debye-type spectral density, Eq. (28), is employed with $\lambda = 0.5$ and $\omega_c = 1$ at $T = 0.5$. (b) Result for the Hamiltonian $\hat{H}_S$ given by Eq. (9) with $\Delta = -0.5$ when the initial condition is $P_1(0) = P_2(0) = 0$ and $P_3(0) = P_4(0) = 1/2$, where other calculation parameters are the same as in (a). (c) Result for the Hamiltonian $\hat{H}_S$ plus $\hat{H}_W$ with $\Delta = -0.5$ and $\delta = 0.5$ when the initial condition is $P_1(0) = P_2(0) = P_3(0) = P_4(0) = 1/4$, where other calculation parameters are the same as in (a). (d) Result for the Hamiltonian $\hat{H}_S$ plus $\hat{H}_M$ with $\Delta = -0.5$ and $\delta = 0.5$ when the initial condition is $P_1(0) = P_2(0) = P_3(0) = P_4(0) = 1/4$, where other calculation parameters are the same as in (a).

players tend to prefer the cooperation when they do not know the opponent's decision; the time-averaged probability of the defection falls below the range spanned by the two limiting cases of knowing the opponent's actions.

To see the underlying mechanisms for this violation of the sure thing principle in more details, we show in Fig. 7 the temporal evolutions of the off-diagonal elements of density matrices calculated for the four cases studied above, as addressed in Figs. 5 and 6. Due to the presence of off-diagonal elements of system Hamiltonians, there appear the off-diagonal elements of density matrices associated with the quantum interference effects. Fig. 8 then illustrates the temporal evolutions of thermodynamic functions of quantum systems, again indicating the dissipative quantum dynamics driven by the free energy decreasing toward the thermodynamic equilibrium value. Interestingly, the entropy shows significant temporal decreases in the cases of the additions of $\hat{H}_W$ (by 28%) and $\hat{H}_M$ (by 44%) as well as those for $\hat{H}_0$ and $\hat{H}_1$, indicating the emergence of correlated order in quantum decision making. The associated entanglement entropy also shows analogous behaviors. These combined effects, in addition to the "wishful thinking" effect embodied by Eq. (10), would account for the realization of the violation of the sure thing principle in the PD problem.

4. Conclusions

In this work we have proposed a computational scheme to describe the quantum dynamics of human decision making represented by the PD problem, in which the action choices by two players are modeled as entangled states interacting with environmental DOF. Through explicit numerical calculations for a general PD problem, we have found a dynamical transition from an arbitrary initial state to the final thermodynamically equilibrium state. Thus, when we start with the Nash equilibrium state for which the both players prefer the defection, the final state governed by the total system Hamiltonian accounting for the payoffs of two players primarily prefers a Paretian optimal state for which the both players favor the cooperation due to the energetic stabilization. Since the quantum coherence effects are taken into account appropriately, the decisions of the players often show the temporal oscillations of quantum beating whose appearance

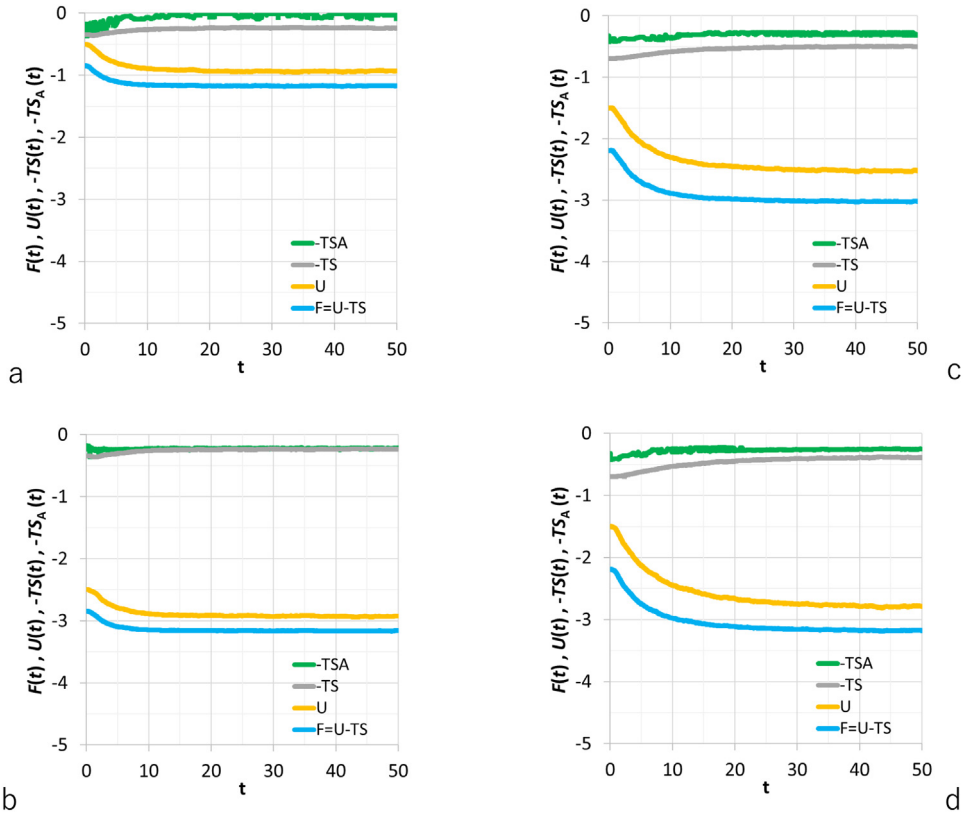

Fig. 8. Temporal evolutions of the thermodynamic functions concerning the violation of the sure thing principle. Yellow, gray, blue and green lines refer to the calculated results for the internal energy $U(t)$, the von Neumann entropy $S(t)$ (times $-T$), the Helmholtz free energy $F(t)$ and the entanglement entropy $S_A(t)$ (times $-T$), respectively. (a) Result for the Hamiltonian $\hat{H}_S$ given by Eq. (9) with $\Delta = -0.5$ when the initial condition is $P_1(0) = P_2(0) = 1/2$ and $P_3(0) = P_4(0) = 0$, where the Debye-type spectral density, Eq. (28), is employed with $\lambda = 0.5$ and $\omega_c = 1$ at $T = 0.5$. (b) Result for the Hamiltonian $\hat{H}_S$ given by Eq. (9) with $\Delta = -0.5$ when the initial condition is $P_1(0) = P_2(0) = 0$ and $P_3(0) = P_4(0) = 1/2$, where other calculation parameters are the same as in (a). (c) Result for the Hamiltonian $\hat{H}_S$ plus $\hat{H}_W$ with $\Delta = -0.5$ and $\delta = 0.5$ when the initial condition is $P_1(0) = P_2(0) = P_3(0) = P_4(0) = 1/4$, where other calculation parameters are the same as in (a). (d) Result for the Hamiltonian $\hat{H}_S$ plus $\hat{H}_M$ with $\Delta = -0.5$ and $\delta = 0.5$ when the initial condition is $P_1(0) = P_2(0) = P_3(0) = P_4(0) = 1/4$, where other calculation parameters are the same as in (a).

depends on the parametrical conditions employed in the computations. It is then essential that these dynamical behaviors are thermodynamically driven by the principle of minimal free energy, and the associated entropy sometimes shows a temporal decrease due to the emergence of correlated order or the preference for specific decision. Summarizing, given the system Hamiltonian to represent the payoffs of the players (diagonal elements) and the quantum interference between the both players' decisions (off-diagonal elements), the present theoretical formulation could provide an unambiguous and comprehensive modeling framework for quantum decision making in a statistical–mechanically consistent manner.

We can also demonstrate an example of the violation of the sure thing principle by investigating the temporal behaviors of the decision of one player when he/she knows or does not know the decision of another player. While the "wishful thinking" mechanism plays a significant role to account for the experimental facts, the consideration of quantum interference effects expressed by the inclusion of inter-state couplings is also important, which is consistent with the findings in earlier works [4,7,23]. Starting with the initial state that the player does not have any information about the opponent's decision and has no preference of own decision, his/her decision goes toward a thermodynamically stable state along with the temporal decrease of free energy and associated decrease of entropy. The probability of defection consequently becomes lower than that for the cases in which the player knows the opponent's decision.

From a conceptual point of view, one may wonder the use of quantum theory for the description of such a macroscopic phenomenon as human decision making. It is essential in this context that we employed the "atomic units" when we borrowed the physical model that describes the quantum phenomena in molecular systems. By setting $\hbar = k_B = 1$, we have reinterpreted the scales of energy, temperature, frequency, time and other physical quantities in the system, so that we have only borrowed the mathematical framework of *quantum logic*, which may be represented by the use of the Liouville–von Neumann equation without $\hbar$ in Eq. (16). The rationale for this interpretation may be (or may not be) traced to a possibility of intimate connection between the macroscopic psychological phenomena and the underlying microscopic quantum physics associated with the working mechanisms of brain and consciousness [48–50], which could

provide attractive topics in future research. Additionally, in a related context, a mathematical similarity between the deep neural network [51] and quantum mechanics is also interesting.

CRediT authorship contribution statement

Shigenori Tanaka: Conceptualization, Methodology, Software, Validation, Formal analysis, Investigation, Resources, Data curation, Writing – original draft, Review & editing, Supervision, Project administration, Funding acquisition. **Toshihito Umegaki:** Methodology, Software, Validation, Formal analysis, Investigation, Data curation, Writing – review & editing, Visualization. **Akihiro Nishiyama:** Methodology, Software, Validation, Investigation, Writing – review & editing. **Hirotaka Kitoh-Nishioka:** Methodology, Software, Validation, Formal analysis, Investigation, Writing – review & editing.

Declaration of competing interest

The authors declare that they have no known competing financial interests or personal relationships that could have appeared to influence the work reported in this paper.

Data availability

The data that support the findings of this study are available from the corresponding author upon reasonable request.

Acknowledgments

We would like to acknowledge the Grants-in-Aid for Scientific Research (Nos. 17H06353, 18K03825 and 21K06098) from the Ministry of Education, Culture, Sports, Science, and Technology (MEXT), Japan, and MEXT Quantum Leap Flagship Program (Grant No. JPMXS0120330644). We also thank Prof. Tomotoshi Nishino at Kobe University for insightful discussion, and Prof. Jerome Busemeyer and Dr. Qizi Zhang for helpful comments on the manuscript.

Appendix A. Supplementary data

Comparisons among various computational schemes to describe the dynamics of open quantum systems are given in Supplementary Material, along with underlying theoretical backgrounds.

Supplementary material related to this article can be found online at https://doi.org/10.1016/j.physa.2022.127979.

References

[1] I. Gilboa, Theory of Decision under Uncertainty, Cambridge University Press, 2009.
[2] E. Shafir, A. Tversky, Thinking through uncertainty - nonconsequential reasoning and choice, Cogn. Psychol. 24 (1992) 449–474.
[3] A. Tversky, E. Shafir, The disjunction effect in choice under uncertainty, Psychol. Sci. 3 (1992) 305–309.
[4] J.R. Busemeyer, P.D. Bruza, Quantum Models of Cognition and Decision, Cambridge University Press, 2012.
[5] E.M. Pothos, J.R. Busemeyer, Quantum cognition, Annu. Rev. Psychol. 73 (2022) 749–778.
[6] J.R. Busemeyer, Z. Wang, J.T. Townsend, Quantum dynamics of human decision-making, J. Math. Psych. 50 (2006) 220–241.
[7] E.M. Pothos, J.R. Busemeyer, A quantum probability explanation for violations of 'rational' decision theory, Proc. Royal Soc. B-Biol. Sci. 276 (2009) 2171–2178.
[8] P.D. Bruza, Z. Wang, J.R. Busemeyer, Quantum cognition: a new theoretical approach to psychology, Trends Cogn. Sci. 19 (2015) 383–393.
[9] J.B. Broekaert, J.R. Busemeyer, E.M. Pothos, The disjunction effect in two-stage simulated gambles: an experimental study and comparison of a heuristic logistic, Markov and quantum-like model, Cogn. Psychol. 117 (2020) 101262.
[10] D.A. Meyer, Quantum strategies, Phys. Rev. Lett. 82 (1999) 1052–1055.
[11] J. Eisert, M. Wilkens, M. Lewenstein, Quantum games and quantum strategies, Phys. Rev. Lett. 83 (1999) 3077–3080.
[12] T. Cheon, T. Takahashi, Interference and inequality in quantum decision theory, Phys. Lett. A 375 (2010) 100–104.
[13] T. Cheon, I. Tsutsui, Classical and quantum contents of solvable game theory on Hilbert space, Phys. Lett. A 348 (2006) 147–152.
[14] V.I. Yukalov, D. Sornette, Quantum decision theory as quantum theory of measurement, Phys. Lett. A 372 (2008) 6867–6871.
[15] V.I. Yukalov, Evolutionary processes in quantum decision theory, Entropy 22 (2020) 681.
[16] A. Khrennikov, A model of quantum-like decision-making with applications to psychology and cognitive science, Biosystems 95 (2009) 179–187.
[17] M. Asano, I. Basieva, A. Khrennikov, M. Ohya, Y. Tanaka, Quantum-like generalization of the Bayesian updating scheme for objective and subjective mental uncertainties, J. Math. Psych. 56 (2012) 166–175.
[18] P.M. Agrawal, R. Sharda, Quantum mechanics and human decision making, Soc. Sci. Res. Netw. Electron. J. (2010) 1–49.
[19] A.O. Caldeira, A.J. Leggett, Path integral approach to quantum Brownian-motion, Physica A 121 (1983) 587–616.
[20] V. May, O. Kuhn, Charge and Energy Transfer Dynamics in Molecular Systems, third ed., Wiley-VCH, Weinheim, 2011.
[21] H. Hossein-Nejad, G.D. Scholes, Energy transfer, entanglement and decoherence in a molecular dimer interacting with a phonon bath, New J. Phys. 12 (2010) 065045.
[22] M. Asano, M. Ohya, Y. Tanaka, I. Basieva, A. Khrennikov, Quantum-like model of brain's functioning: Decision making from decoherence, J. Theoret. Biol. 281 (2011) 56–64.
[23] I. Martinez-Martinez, E. Sanchez-Burillo, Quantum stochastic walks on networks for decision-making, Sci. Rep. 6 (2016) 23812.
[24] J. Broekaert, I. Basieva, P. Blasiak, E.M. Pothos, Quantum-like dynamics applied to cognition: A consideration of available options, Proc. R. Soc. Lond. Ser. A Math. Phys. Eng. Sci. 375 (2017) 20160387.
[25] J. Busemeyer, Q. Zhang, S.N. Balakrishnan, Z. Wang, Application of quantum-Markov open system models to human cognition and decision, Entropy 22 (2020) 990.

[26] A. Rosner, I. Basieva, A. Barque-Duran, A. Glockner, B. von Helversen, A. Khrennikov, E.M. Pothos, Ambivalence in decision making: An eye tracking study, Cogn. Psychol. 134 (2022) 101464.
[27] S.J. Cotton, W.H. Miller, Symmetrical windowing for quantum states in quasi-classical trajectory simulations: Application to electronically non-adiabatic processes, J. Chem. Phys. 139 (2013) 234112.
[28] S.J. Cotton, W.H. Miller, The symmetrical quasi-classical model for electronically non-adiabatic processes applied to energy transfer dynamics in site-exciton models of light-harvesting complexes, J. Chem. Theory Comput. 12 (2016) 983–991.
[29] W.H. Miller, S.J. Cotton, Communication: Wigner functions in action–angle variables, bohr-sommerfeld quantization, the heisenberg correspondence principle, and a symmetrical quasi-classical approach to the full electronic density matrix, J. Chem. Phys. 145 (2016) 081102.
[30] K. Friston, A free energy principle for biological systems, Entropy 14 (2012) 2100–2121.
[31] J. Sanchez-Canizares, The free energy principle: Good science and questionable philosophy in a grand unifying theory, Entropy 23 (2021) 238.
[32] A. Ishizaki, G.R. Fleming, Unified treatment of quantum coherent and incoherent hopping dynamics in electronic energy transfer: Reduced hierarchy equation approach, J. Chem. Phys. 130 (2009) 234111.
[33] A. Ishizaki, G.R. Fleming, Theoretical examination of quantum coherence in a photosynthetic system at physiological temperature, Proc. Natl. Acad. Sci. USA 106 (2009) 17255–17260.
[34] Y. Suzuki, H. Watanabe, Y. Okiyama, K. Ebina, S. Tanaka, Comparative study on model parameter evaluations for the energy transfer dynamics in fenna-matthews-olson complex, Chem. Phys. 539 (2020) 110903.
[35] Y. Suzuki, K. Ebina, S. Tanaka, Four-electron model for singlet and triplet excitation energy transfers with inclusion of coherence memory, inelastic tunneling and nuclear quantum effects, Chem. Phys. 474 (2016) 18–24.
[36] J.E. Runeson, J.O. Richardson, Spin-mapping approach for nonadiabatic molecular dynamics, J. Chem. Phys. 151 (2019) 044119.
[37] J.E. Runeson, J.O. Richardson, Generalized spin mapping for quantum–classical dynamics, J. Chem. Phys. 152 (2020) 084110.
[38] T. Kadowaki, H. Nishimori, Quantum annealing in the transverse ising model, Phys. Rev. E 58 (1998) 5355–5363.
[39] H.-D. Meyer, W.H. Miller, A classical analog for electronic degrees of freedom in nonadiabatic collision processes, J. Chem. Phys. 70 (1979) 3214–3223.
[40] H. Wang, X. Song, D. Chandler, W.H. Miller, Semiclassical study of electronically nonadiabatic dynamics in the condensed-phase: Spin-boson problem with debye spectral density, J. Chem. Phys. 110 (1999) 4828–4840.
[41] P.L. Walters, T.C. Allen, N. Makri, Direct determination of discrete harmonic bath parameters from molecular dynamics simulations, J. Comput. Chem. 38 (2017) 110–115.
[42] C.J.S. Sandoval, A. Mandal, P.F. Huo, Symmetric quasi-classical dynamics with quasi-diabatic propagation scheme, J. Chem. Phys. 149 (2018) 044115.
[43] M. Kian, M.W. Alomari, Klein's trace inequality and superquadratic trace functions, 2019, 2019120192, http://dx.doi.org/10.20944/preprints201912.0192.v2, Preprints.
[44] S. Tanaka, Diffusion Monte Carlo study on temporal evolution of entropy and free energy in nonequilibrium processes, J. Chem. Phys. 144 (2016) 094103.
[45] P. Calabrese, J. Cardy, B. Doyon, Entanglement entropy in extended quantum systems introduction, J. Phys. A 42 (2009) 500301.
[46] J. Eisert, M. Cramer, M.B. Plenio, Colloquium: Area laws for the entanglement entropy, Rev. Modern Phys. 82 (2010) 277–306.
[47] J. Provazza, D.F. Coker, Communication: Symmetrical quasi-classical analysis of linear optical spectroscopy, J. Chem. Phys. 148 (2018) 181102.
[48] K.H. Pribram, K. Yasue, M. Jibu, Brain and Perception: Holonomy and Structure in Figural Processing, Psychology Press, 1991.
[49] S. Hameroff, R. Penrose, Orchestrated reduction of quantum coherence in brain microtubules: A model for consciousness, Math. Comput. Simulation 40 (1996) 453–480.
[50] A. Nishiyama, S. Tanaka, J.A. Tuszynski, Non-equilibrium quantum brain dynamics II: Formulation in 3+1 dimensions, Physica A 567 (2021) 125706.
[51] N. Cohen, O. Sharir, A. Shashua, On the expressive power of deep learning: A tensor analysis, Proc. Mach. Learn. Res. 49 (2016) 698–728.